Coordinated Control and Range Imaging for Mobile Manipulation

Dean Anderson, Thomas M. Howard, David Apfelbaum, Herman Herman, and Alonzo Kelly

Robotics Institute
Carnegie Mellon University
5000 Forbes Ave, Pittsburgh PA 15213
{dranders,thoward,da0g,h.herman,alonzo}@ri.cmu.edu

1 Introduction

Mobile manipulators currently deployed for explosive ordinance disposal are typically controlled via crude forms of teleoperation. Manipulator joints are actuated individually in joint space, making precise motions in state space difficult. Scene understanding is limited, as monocular cameras provide little (if any) depth information. Furthermore, the operator must manually coordinate the manipulator articulation with the positioning of the mobile base. These limitations place greater demands on the operator, decrease task efficiency and can increase exposure in dangerous environments.

In this paper, we demonstrate several enabling technologies for interacting with and operating mobile manipulators, including a "click-and-grab" interface for coordinated motion and manipulation. This includes coordinated joint movement for end-effector position control, a flash LADAR to provide depth information, and automatic trajectory generation to autonomously position the mobile base and manipulator.

1.1 Related Work

Related work for this paper spans mobile manipulator design, motion planning, sensing, and applications. Currently, several commercial robotic platforms are sold and deployed for EOD and USAR applications. Foster-Miller's TALON platform and iRobot's PackBot [11] are among the most popular. Both vehicles are skid-steered, tracked vehicles equipped with a manipulator arm. Visual feedback for such systems is provided by multiple color cameras.

The primary deficiency of such platforms is the lack of autonomous capabilities within the operator interface. The manipulator arms are controlled in the joint-velocity space with no direct measure of end effector position provided to the operator. Cameras provide extremely limited depth information, requiring the operator to “feel” for the object with the end effector.

In the more general area of mobile manipulators the systems and levels of autonomy are more varied. For motion planning of high degree of freedom systems, the elastic strip method in [1] modifies a path in the workspace of the vehicle to achieve real-time obstacle avoidance. Simulated annealing was used to solve the global optimization problem of task planning for a mobile manipulator in [2]. Desai and Kumar [3] applied calculus of variations to accommodate geometric, kinematic, and dynamics constraints to solve the multi-robot coordination problem for a pair of mobile manipulators. Galicki [4] proposed a local velocity perturbation technique to avoid singularities and obstacles. Manipulator and base trajectory generation are treated as a single unified boundary state constraint satisfaction problem in [10]. This paper expands on this work by extending the model-predictive trajectory generation technique from [6] to satisfy the manipulator and base state constraints.

Our work is distinct from the prior art in three areas. First, we utilize a registered range imager to provide the operator visual, as well as depth information. Second, we utilize the range information to automatically plan a path based on a targets position. Lastly, we provide an intuitive interface for manipulating and controlling the robot and leverage autonomy to minimize operator workload.

2 System Description

The host platform for these experiments was a modified LAGR mobile robot [7], fitted with a custom three degree-of-freedom manipulator arm and a gripper end-effector(Figure 1). It is similarly scaled to currently fielded EOD robots and its differential drive is analogous to tracked, skid-steered vehicles. The base vehicle has proved to be a very flexible research platform: in addition to over 40 standard models deployed at various universities, custom versions with LADAR, metal detectors and omni-directional cameras have been built.

The manipulator used is a custom-built, 3-DOF anthropomorphic-arm, with a gripper end effector. The shoulder yaw joint is powered by a harmonic-drive motor. The shoulder and elbow pitch joints consist of Smart Motors fitted with gearboxes, brakes and relative encoders. Each joint in the manipulator is speed limited to 18 deg/s.

The perception system on the vehicle consists of two color video cameras, and a flash LADAR unit provided by PMDtec[8]. One camera is mounted on the manipulator arm near the wrist, for use during manipulation. The second camera and flash LADAR unit is mounted to the shoulder yaw joint for driving and target acquisition. A close up view of this sensor package is shown in Figure 1b.

(a) (b)

Fig. 1. (a) Modified LAGR mobile robot with 3-DOF manipulator arm and a 1-DOF end effector. 1(b) the color and flash LADAR sensor package.

Unlike traditional LADAR, which must be mechanically scanned, flash LADAR measures a full 2D array of depth information in a single frame (Figure 2). The PMDtec sensor integrated into the LAGR-EOD had a 30 Hz framerate, a 64x48 pixel array, a maximum range of 7.5 m, and was capable of operation in indoor and outdoor environments. The field of view was adjustable using standard C-mount optical lenses. For our experiments, a lens with a focal length of 4.2mm was used. This provided a 60 degrees horizontal and vertical field of view.

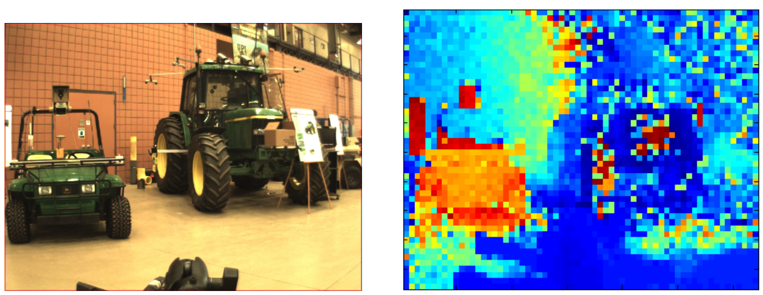

(a) (b)

Fig. 2. Corresponding output from the color camera (a) and flash LADAR (b).

3 Technical Approach

This section covers the algorithms used to develop the intelligent teleoperated mobile manipulator system. Section 3.1 covers the technologies for intelligent teleoperation, including co-registration, the “click and grab” interface, end effector depth perception, and the motion and grasp planning systems. Section 3.2 covers the automated workspace extension, a simpler interface for teleoperation controls for coordinated motion and manipulation.

3.1 Intelligent Teleoperation

Click and Grab

“Click and grab” is a system for automating simple manipulation tasks. Rather than requiring the operator to manually position the vehicle and control the arm to manipulate the target, the operator simply clicks on the desired target in a color image. The system then uses range information to autonomously plan and execute a path to grab the target.

Operator Control Station

The operator control station (OCS) is the main software package for intelligent teleoperation of the system. The software runs on a single external notebook computer with additional inputs provided through a gaming-type control pad with dual two-axis analog joysticks and multiple buttons.

The OCS consists of two main panels: the image viewing and control panel (Figure 3a) and the plan preview and adjustment panel (Figure 3b). The image viewing panel is where the operator designates a target by clicking on an image, switches cameras or control modes, and monitors vehicle status. The plan preview panel allows the operator to view a real-time simulation of the vehicle before execution of a potential trajectory. The operator can override the motion planner by adjusting the path shape in this panel.

Co-Registration and Click Interface

A critical component of the “click and grab” interface is the ability to recover a 3D point in the workspace from pixel coordinates in the color image. This was achieved by co-registering the flash LADAR to the color camera by computing the homogeneous transform between the LADAR and camera frames, and finding the 3D range point which best matches the clicked image coordinates.

While a projective lens model can directly map a point in 3D space to image coordinates, the inverse, mapping image coordinates to a 3D point, is not so straightforward. Each pixel in an image corresponds to an entire ray. Therefore, it is necessary to perform a search along that ray to find the best 3D point in the range image corresponding to the clicked point in the color image. Because of the relatively small number of range pixels, we simply exhaustively test each point, but the search could be confined to the epipolar line, similar to stereo matching algorithms.

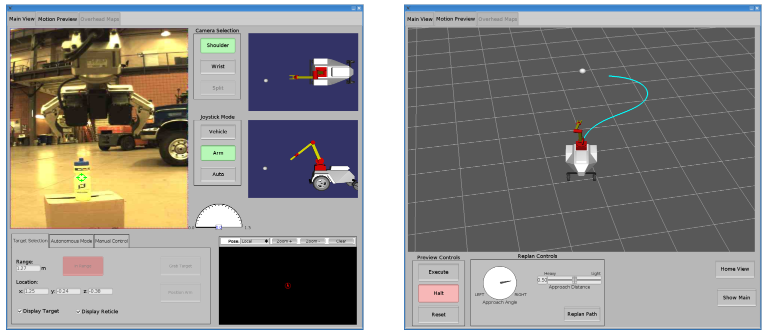

(a) (b)

Fig. 3. The main Operator Control Station (OCS) and path preview interfaces are shown in (a) and (b) respectively. The OCS provides windows for camera and configuration feedback and task oriented controls. The path preview interface shows the output from the motion planner and provides controls to adjust the path shape.

Points are tested by transforming them from the LADAR to the camera frame via the transform, and then projecting them into image coordinates using a projective lens model. The point closest to the clicked pixel, within some minimum threshold of projection error, is selected as the best match.

End Effector Depth Perception

During early testing, it was determined that depth perception is critical to end effector performance during teleoperation. A simple system we employed was to mount a laser pointer within the gripper and place a scaled overlay on the video feed from the wrist camera. Due to the epipolar geometry, the pointer's position along scale corresponds to the distance from the gripper. We were then able to calibrate a target reticle to allow the operator to know when the target was within grasping range (Figure 4).

This greatly improves an operators ability to grasp and manipulate objects. Instead of having to "feel" for the object to determine whether it is in grasping range, there is direct visual feedback.

Motion Planning

The motion planner developed to generate paths from the current state to the target vehicle state followed the methodology outlined in [5]. An expressive search space is generated by intelligently sampling the state space of terminal vehicle configurations based on feasible base placements for the mobile manipulator. A feasible base placement is defined as a vehicle position and orientation where the manipulation target is within the workspace of the manipulator.

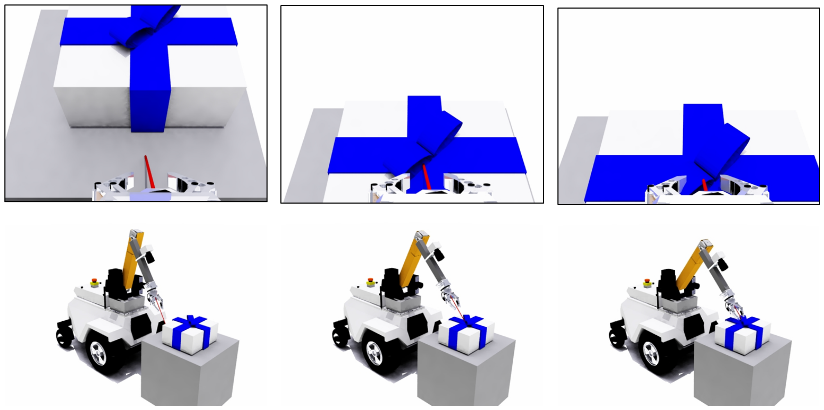

(a) (b) (c)

Fig. 4. Utilizing the laser guide and video overlay for monocular depth measurement. (a) Initial configuration. (b) Aligning end-effector with the target. (c) Moving end-effector in range.

The model-predictive trajectory generation algorithm from [6] is applied to generate each action in the search space. This algorithm is well suited to this application as it can handle arbitrary terrain, predictive motion models, and produce smooth, continuous trajectories between arbitrary boundary state pairs. Since the predictive motion model in the trajectory generator includes the motion of the manipulator, conditions including tip-over and collision can be estimated and avoided.

The terminal boundary state constraint vector includes vehicle position (x, y) and orientation (ψ), along with the manipulator and end effector configuration $(\mathbf{c_m}, \mathbf{c_{ee}})$:

$$\mathbf{x_C} = \left[\, x \; y \; \psi \; \mathbf{c_m} \; \mathbf{c_{ee}} \,\right]^T \tag{1}$$

The configuration constraints on the manipulator or end effector are expressed in the state space, although in general they could be defined in the joint space. To generate actions between the boundary state pair, a set of parameterized vehicle controls, which include functions to describe the motion of the end effectors, were used:

$$\mathbf{u}(\mathbf{p}, \mathbf{x}) = \left[\, v_x(\mathbf{p}, \mathbf{x}) \; \kappa(\mathbf{p}, \mathbf{x}) \; x_{ee}(\mathbf{p}, \mathbf{x}) \; y_{ee}(\mathbf{p}, \mathbf{x}) \; z_{ee}(\mathbf{p}, \mathbf{x}) \,\right]^T \tag{2}$$

The manipulator's control inputs are defined as parameterized functions of the target end effector relative 3D position $(x_{ee}(\mathbf{p}, \mathbf{x}), y_{ee}(\mathbf{p}, \mathbf{x}), z_{ee}(\mathbf{p}, \mathbf{x}))$, similar to the way that workspace controls are used. Parameterized function of individual manipulator joint angles could be used in lieu of the end effector 3D position.

The sampling strategy for the base placement is important to the performance of the motion planner. The end effector position (the manipulation target) is fully defined in the world frame but the vehicle position, orientation, and manipulator configuration can vary significantly. Consider the two sampling strategies exhibited in Figure 5. The nonholonomic constraints of differential-drive vehicles can have significant effects on the shape of the trajectory required to reach a terminal pose. The shoulder yaw joint can compensate for a vehicle orientation not aligned with the manipulation target.

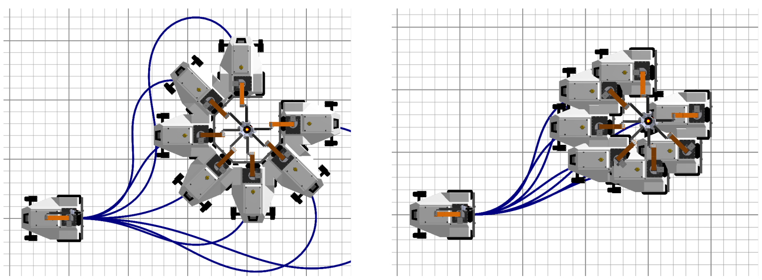

(a) (b)

Fig. 5. Examples of possible variations in base placement for reaching a manipulation target. In (a), vehicle position is sampled while keeping relative heading between the target and the vehicle constant, while in (b) absolute vehicle heading is kept constant.

3.2 Automated Workspace Extension

Workspace Controls

The kinematics of multiple-link manipulators has been well studied for over 40 years. Sciavicco and Siciliano in [9] discuss the modeling and control of such manipulators. Of particular interest to this work, is the notion of differential kinematics. By computing and inverting the manipulator Jacobian, it is possible to map a velocity vector in Cartesian space to a vector in joint space.

This allows the operator to specify desired motions directly in the manipulation workspace, and allows for a more intuitive control scheme. The coordinate system can also be chosen to maximize task efficiency. For example, the control frame could be attached to the wrist camera, whereby one control axis moves the camera forward and backwards, and the other axes pan and tilt the camera left, right, up and down. This would allow the operator essentially "drive" the manipulator from a first-person perspective. Other choices for control frames include polar base-frame coordinates or the vehicle Cartesian frame.

Automatic Workspace Extension

An additional benefit of having a mobile manipulator is the ability to extend the manipulation workspace by moving the vehicle. Furthermore, operator workload can be reduced by doing so automatically when a manipulation command would exceed the workspace. An example of this can be seen in Figure 6, where the operator commands the end effector forward to reach a target that is well outside the reach of the manipulator arm. This relaxes the precision with which the operator must position the vehicle before beginning manipulation.

In our current system, we command the vehicle to move at a rate equal to the component of end-effector velocity along the vehicle forward axis. Due to the non-holonomic constraints, we do not extend the workspace in the lateral (robot-frame) directions. It may be possible to also adjust the vehicle heading to do so, but such motions may have undesirable results in terms of vehicle base placement in constrained, or sensitive environments.

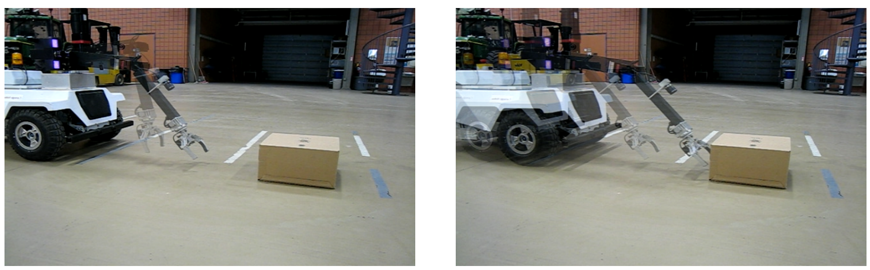

(a) (b)

Fig. 6. Images showing automatic workspace expansion. In (a), the manipulator moves the end-effector along the vehicle forward axis to the edge of the workspace. In (b), the vehicle moves forward in response to the same manipulator command, effectively extending the workspace of the manipulator.

4 Experimental Design

The sets of experiments fall into two categories, robustness tests to evaluate the accuracy of the coordinated motion planning and control, and an informal user study to evaluate the effectiveness of the autonomous system in terms of increasing efficiency and usability. The test platform was a modified LAGR mobile robot retrofitted with a custom three-joint manipulator with a single degree of freedom end effector (Fig 1a).

For the planning test, the system planned and then executed a series of trajectories to several points at different headings. The vehicle's final pose after execution, as measured by the on-board IMU, was then compared to the planned terminal pose.

The user study asked the operator to perform a simple manipulation task, in this case picking up a water-bottle, in two different scenarios. The first scenario had the target beyond the manipulator's workspace, requiring the operator to move and position the vehicle before manipulation could begin. The second scenario had the operator pick up the water-bottle using both joint-space and work-space control, from a static position. In both scenarios, time to completion was measured, and any errors, such as knocking over the bottle, were recorded.

5 Results

Autonomous Base Placement

Fifteen different trajectories, comprising three different terminal positions with five different terminal headings, were planned and executed. The planned paths ranged in distance from 6.5 m to 16 m. The resulting terminal position error averaged 0.21 m, or when normalized by path length, 0.02 meter per meter traversed. RMS orientation error averaged 11.3 degrees. The magnitudes of these errors are sufficiently small that they can be (automatically) compensated for by the manipulator, however they could be further reduced using feedback in the control and vehicle model identification.

Operator Efficiency

The user study demonstrated that the automatic manipulation system was at least comparable to a human operator in both accuracy and speed. On average, the automatic click and grab system was able to perform the static manipulation task 13% faster than the users (Table **??**). However, it completed the driving task an average of 25% slower, largely due to range measurement error and replanning.

Work-space controls reduced both the time required to complete the task as well as the number of errors made. On average across four trials, operators reduced their number of errors from three to one, and reduced their completion time by 11%. The results demonstrate that the autonomy and perceptive capabilities of our system eases the workload on the operator while increasing task efficiency.

Results from the automatic system were potentially limited by the accuracy of the flash LADAR range and co-registration. At short ranges, accuracy was sufficient to reliably grasp an object. However, at longer ranges, errors were large enough to cause manipulation errors. Instead, “click and grab” at long range required several operator interventions to re-designate the target once the base had positioned itself within range.

6 Conclusions

In this work, we have successfully demonstrated the utility of increased autonomy and intelligence in teleoperated robotic platforms, such as those currently being used for Explosive Ordinance Demolition (EOD). In particular, switching from a joint-space control scheme to one which operates in workspace allows for finer control is potentially reduced learning curves. It is also a technology that can easily incorporated into the current generation of EOD robots.

Finally, robotic autonomy has also been shown to potentially reduce operator workload and increase task efficiency. Instead of constantly teleoperating the vehicle, with autonomy the operator can simply set it and forget it: designating a target and then performing other tasks while the robot autonomously performs the task.

References

1. Brock, O., Khatib, O., Viji, S.: Elastic strips: A framework for motion generation in human environments. International Journal of Robotics Research **21**(12), 1031–1052 (2002)
2. Carriker, W., Khosla, P., Krogh, B.: Path planning for mobile manipulators for multiple task execution. IEEE Transactions on Robotics and Automation pp. 403 – 408 (1991)
3. Desai, J., Kumar, V.: Nonholonomic motion planning for multiple mobile manipulators (1997). URL citeseer.ist.psu.edu/desai97nonholonomic.html
4. Galicki, M.: Inverse kinematic solution to mobile manipulators. International Journal of Robotics Research **22**(12), 1041–1064 (2003)
5. Howard, T., Green, C., Ferguson, D., Kelly, A.: State space sampling of feasible motions for high performance mobile robot navigation in complex environments. Journal of Field Robotics **25**(6-7), 325–345 (2008)
6. Howard, T., Kelly, A.: Optimal rough terrain trajectory generation for wheeled mobile robots. International Journal of Robotics Research **26**(2), 141–166 (2007)
7. Jackel, L., Krotkov, E., Perschbacher, M., Pippine, J., Sullivan, C.: The DARPA LAGR program: Goals, challenges, methodology, and phase I results. Journal of Field Robotics **23**, 945–973 (2006)
8. Möller, T., Kraft, H., Frey, J., Albrech, M., Lange, R.: Robust 3D measurement with pmd sensors. In: Proceedings of the First Range Imaging Research Dat at ETH Zurich (2005). ISBN 3-906467-57-0
9. Sciavicco, L., Sciliano, B.: Modeling and Control of Robot Manipulators. Springer-Verlag (2000)
10. Seraji, H.: A unified approach to motion control of mobile manipulators. The International Journal of Robotics Research **17**(2), 107–118 (1998)
11. Snyder, R.G.: Robots assist in search and rescue efforts at wtc. IEEE Robotics and Automation Magazine pp. 26–28 (2001)